Electrochimica Acta 78 (2012) 557–562

Contents lists available at SciVerse ScienceDirect

Electrochimica Acta

journal homepage: www.elsevier.com/locate/electacta

A scanning electrochemical microscopy procedure for micropatterning Al_2O_3-thin films deposited on a platinum substrate

Dario Battistel, Salvatore Daniele*,[1], Davide Fratter

Dipartimento di Scienze Molecolari e Nanosistemi Università Cà Foscari Venezia, Calle Larga, S. Marta, 2137, 30123 Venice, Italy

ARTICLE INFO

Article history:
Received 5 January 2012
Received in revised form 15 June 2012
Accepted 18 June 2012
Available online 30 June 2012

Keywords:
Patterning
Scanning electrochemical microscopy
Focusing
Alumina
Platinum

ABSTRACT

A scanning electrochemical microscopy (SECM) procedure for patterning alumina thin films deposited onto a platinum film (Pt/Al_2O_3) was investigated. The alumina surface was locally etched by hydroxide ions, which were generated at platinum microelectrodes, by exploiting the hydrogen evolution process in aqueous solutions. The local base-induced dissolution of Al_2O_3 to soluble AlO_2^- species allowed the exposure of the underlying platinum, which resulted in well-defined conducting spots embedded within an insulating matrix. Reproducibility of the spots was achieved by adding to the electrolyte solutions amounts of EDTA, which acted as a scavenger for OH^- ions, while allowed the complexation of the aluminium ions formed at the sample surface during the wet etching process. The effects of electrolysis time, tip to substrate distance and overall tip dimension on the shape and size of the conducting spots were investigated in detail. Furthermore, the possibility to create complex patterns with the optimised etching procedure was also shown.

1. Introduction

The development of technologies for micro- and nano-patterning of materials is a significant area of research, as they allow fabrication of micro- and nano-structures, which have widespread technological applications in a variety of fields, including electronics [1,2], chemical conversion [3,4], magnetic data storage [5] and sensors [6,7]. Most patterning approaches are based on photolithography [8], where a desired pattern is designed and fabricated as a mask and used to transfer the pattern into the material. However, this technique is rather expensive and new techniques and strategies are being developed for patterning purposes. Scanning probe techniques have been used for the generation of micro- and nano-structures by a local control of the surface functionality on either conducting or insulating materials [9]. Among them, scanning electrochemical microscopy (SECM) [10] has proven to be a powerful and rather inexpensive tool for achieving these goals [11]. In SECM experiments, the probe is a microelectrode [12]: it is placed close to a substrate immersed in an electrolytic solution. A current response, due to a redox mediator [10], is recorded at the tip as a function of its z (approach curve) or x–y (scanning) position above the sample [10]. In this way information on reactivity and topography of the substrate can be acquired. In addition, as lithography, SECM can be used to manipulate the surface and generate micro- and nano-structures. Manipulations include deposition of metals [13,14] and polymers [15,16], functionalisation of surface [17–21] and locally removal (etch) part of materials [22–26]. The latter procedure has been employed to create micropits on either metals or semiconductors.

One of the most employed strategies for etching a substrate by SECM involves the generation of an etchant species at the microelectrode. The reactive species diffuses to the sample and reacts therein with the surface material, resulting in a localised pattern. The chemical process that occurs at the solid/solution interfaces depends on the nature of both sample material and etchant species and, in some cases, it is coupled with chemical reactions in the solution. The challenge in these experiments is to bring the fabricated pattern into structures of well-defined shapes and sizes. In fact, for slow kinetics at the interface, the etchant species can diffuse laterally from the microelectrode to the substrate gap. This can generate further etching processes in undesired regions of the surface, thus leading to poor reproducible features of the patterns. This difficulty can be overcome by resorting to the "chemical lens" approach [27,28], in which a scavenger is added to the solution to provide a focusing effect of the etchant species generated at the tip. This enables etching of areas of defined sizes and shapes. This concept has been exploited to pattern a variety of substrates by the use of a number of focusing schemes [13,15,16,27–30].

In this article, we apply the approach of the chemical lens to pattern ceramic thin films by exploiting an acid/base induced erosion process. The method implies the local generation, at the SECM tip, of acid or base challenges consistent with those of acid or base erosion of the material. This results in pits whose sizes and shapes

* Corresponding author. Tel.: +39 041 2348630; fax: +39 041 2348594.
E-mail address: sig@unive.it (S. Daniele).
[1] ISE member.

0013-4686/$ – see front matter © 2012 Elsevier Ltd. All rights reserved.
http://dx.doi.org/10.1016/j.electacta.2012.06.066

depend on several parameters such as tip size, tip to substrate distance (d), and time of electrolysis (t_{el}) producing the etchant species. The acid-induced erosion version has recently been applied for studying stability and erosion rate of minerals such as marble [23] and dental enamel [24] under acid attack. In recent preliminary work [31,32], the local base-induced dissolution process has been applied to investigate the local stability of alumina thin films deposited on a platinum film (Pt/Al_2O_3) [30] and to generate a bipolar system to provide clear evidence for positive feedback limitation during SECM measurements of unbiased conductors [32]. In this paper, details on the base-induced dissolution process for patterning reproducibly Pt/Al_2O_3 samples are provided. Local basicity is achieved by the generation, at a series of platinum microelectrode-SECM tips, of controlled amounts of hydroxide ions, exploiting the hydrogen evolution process:

$$2H_2O + 2e = H_2 + 2OH^- \quad (1)$$

Thus, ultimately, the procedure employed here allows the generation, under an SECM configuration, of conducting platinum microspots embedded within the alumina insulating matrix.

2. Experimental

2.1. Chemicals and samples

Hexaammine ruthenium (III) chloride, potassium chloride and ethylendiamine-tetraacetic acid disodium salt (EDTA) were of reagent grade and purchased from Sigma–Aldrich. They were used as received. All aqueous solutions were prepared using water purified with a Milli-Q system. Target materials, for film preparation by sputtering, were 2 in. diameter Pt (99.99%) and sintered Al_2O_3 (99.99%) disks. Sputtering was performed in pure Ar (99.9995%).

Platinum and alumina thin films were deposited layer by layer on a silicon wafer in a custom-built r.f. magnetron sputtering system as described elsewhere [33]. The thickness of the Pt and Al_2O_3 layer was 380 (±20) and 25 (±3) nm, respectively. They were obtained by examining a cross section of the sample by scanning electron microscopy (SEM). X-ray diffraction measurements showed that the alumina film was amorphous.

2.2. Electrodes and instrumentation

Platinum disk microelectrodes of 25, 20 and 5 μm diameter were employed as SECM tips. They were prepared by sealing platinum wires within a glass capillary [34]. Afterward, they were tapered to a conical shape, polished with graded alumina powder down to 0.3 μm and then characterised by cyclic voltammetry at low scan rates and SECM to evaluate the actual electrode radius of the microelectrode and the overall tip radius to the electrode radius ratio (RG) [10,34]. The tips employed here were characterised by RG values of 5 and 10. The reference electrode was an Ag/AgCl, in saturated KCl, and the counter electrode was a Pt coil. The Pt/Al_2O_3 samples were immobilised at the bottom of the cell by an O-ring.

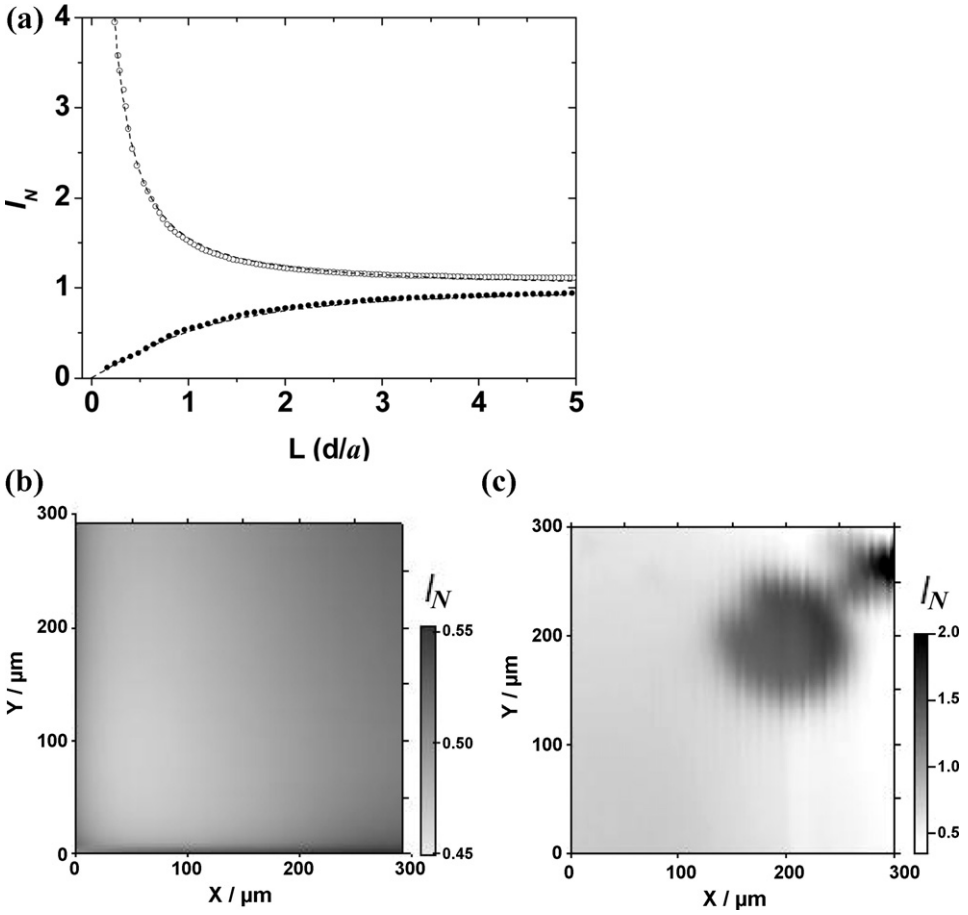

Fig. 1. SECM responses obtained by analysis of a Pt/Al_2O_3 sample, using a Pt microdisk 12.5 μm radius and RG = 10 in an aqueous solution containing 1 mM $Ru(NH_3)_6Cl_3$ + 0.1 M KCl. (a) Normalised current ($I_N = I/I_{bulk}$) against normalised distance ($L = d/a$) (•) before and (○) after etching the sample; lines are diffusion controlled theoretical approach curves. (b) and (c) SECM images recorded before and after, respectively, base-induced etching of the alumina layer for 10 min at d = 5 μm. SECM images were recorded at a scan speed of 10 μm s^{-1}.

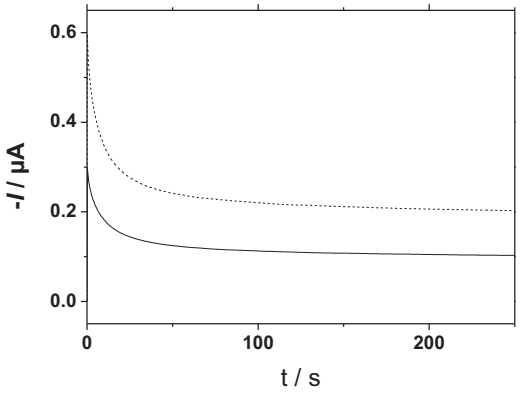

Fig. 2. Chronoamperometry obtained at Pt microdisk 12.5 μm radius positioned at d = 5 μm in an aqueous solution containing 1 mM $Ru(NH_3)_6Cl_3$ + 0.1 M KCl. Applied potential (-) −1.2 V and (—) −1.4 V against Ag/AgCl.

Electrical connection of the samples was achieved by fixing a copper wire at an uncoated edge of the Pt film.

A CHI920B workstation (CH instruments) was employed for voltammetric experiments and for some SECM measurements. A home built SECM apparatus, described in detail elsewhere [31], was also used for etching and performing the analysis of the Pt/Al_2O_3 sample surfaces. All measurements were carried out in a classical three-electrode cell, which was located in a Faraday cage. The base electrolyte consisted of 0.1 M KCl, which was fortified by 1 mM $Ru(NH_3)_6Cl_3$ as redox mediator for surface analysis by SECM and, in most SECM experiments, by different amounts of EDTA to control the pattern features (vide infra). During base-induced etching experiments of the alumina layer, the measurements were performed with the samples kept unbiased; a potential bias of 0.1 V was applied to the samples during SECM analysis of the surfaces. The latter conditions ensured the diffusion controlled regeneration of the redox mediator at the conducting microspots [31]. Diffusion controlled reduction of $Ru(NH_3)_3^{3+}$ at the microelectrode tip was achieved by applying a potential of −0.35 V. Approach curves were plotted using normalised currents, $I_N = I/I_{bulk}$, (I = the actual tip current; I_{bulk} = current measured in the bulk), against normalised distances $L = d/a$ (d = tip-substrate distance; a = electrode radius). Normalised currents were also used for drawing SECM images.

SEM micrographs of the surfaces and cross section of the samples were obtained by a JEOL JMS 5600LV microscope equipped with an EDS electron microprobe for elemental analysis. Atomic force microscopy (AFM) images were performed in tapping mode using a Veeco Digital Instruments D 3100.

3. Results and discussion

3.1. Optimisation of the etching procedure

Preliminarily, the surface status of the alumina layer was monitored by SECM in a neutral KCl solution by performing approach curves and two-dimensional scans (Fig. 1). Fig. 1a, filled circle, and Fig. 1b shows typical SECM responses obtained at a Pt/Al_2O_3 sample before performing any etching operations. As is evident, all types of experiments are characterised by negative feedback responses, due to hindered diffusion of the redox mediator towards the microelectrode surface [10]. This indicates that the substrate is insulating and that no region of the underlying platinum layer is exposed to the electrolyte solution. If the latter situation occurred, positive feedback responses would have been recorded (vide infra). The small changes of normalised current observed above the substrate reflect, conceivably, the surface tilt, which was not corrected before performing the experiments.

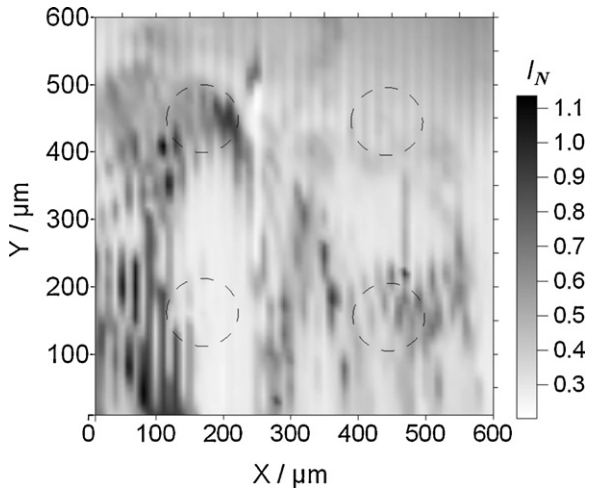

Fig. 3. SECM image obtained after etching the alumina layer for 10 min, using a Pt microdisk 12.5 μm radius (RG = 10), d = 5 μm, in an aqueous solution containing 1 mM $Ru(NH_3)_6Cl_3$ + 0.1 M KCl. Scan speed 10 μm s^{-1}. The etched zones are indicated with circles.

To allow the base-induced etching of the alumina layer, the platinum tip potential was set at values ranging from −1.2 V to −1.4 V. These conditions ensured the generation of large enough amounts of hydroxide ions through reaction (1). As is evident in Fig. 2, sufficiently stable tip currents, with average values varying between 100 and 200 nA, were obtained after about 40 s. These experiments refer to the Pt microelectrode of 12.5 μm radius. Apart from the specific values, a similar behaviour was observed using the 10 and 2.5 μm radius Pt disks. From the average steady-state limiting currents, the OH^- concentration produced at the tip was estimated to be in the range 0.01–0.02 M, which ensured local (i.e., within the tip/substrate gap) pH conditions, such that dissolution of alumina could take place through reaction (2) [31]:

$$Al_2O_3 + 2OH^- = 2AlO_2^- + H_2O \quad (2)$$

Consequently, when sufficiently long electrolysis times were used, the etching operation caused the exposure of the underlying platinum film of the Pt/Al_2O_3 sample beneath the microelectrode. SECM analysis performed after etching, using $Ru(NH_3)_3^{3+}$ as redox mediator, allowed revealing the generated conducting spots. Included in Fig. 1 are typical SECM responses obtained after etching the alumina layer for 4 min and maintaining the 12.5 μm radius tip (RG = 10) at 5 μm above the substrate. As is evident, the approach curve (Fig. 1a open circle) and the SECM image (Fig. 1c) display now higher normalised currents above the etched regions, as expected for the regeneration of the redox mediator at a conducting substrate [10]. To further support these results, experimental approach curves were compared with those predicted by the theory for a diffusion controlled process (lines in Fig. 1a) [35], and the agreement was very good. Although the results proved that, under

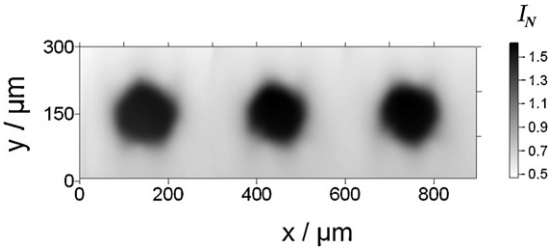

Fig. 4. SECM image obtained after three repeat etches by using a Pt microdisk 12.5 μm radius (RG = 10), d = 5 μm, t_{el} = 10 min in an aqueous solution containing 1 mM $Ru(NH_3)_6Cl_3$ + 0.1 M KCl + 0.07 M EDTA. Scan speed 10 μm s^{-1}.

the above experimental conditions, alumina could be dissolved, the shape of the spots were however scarcely reproducible and badly resolved irrespective of the electrolysis potential and time, as well as the tip-substrate distance. This is shown in Fig. 3, where an SECM image of an attempt to create an array of four platinum conducting spots is displayed. Moreover, etching of the alumina film could also occur in regions outside the tip to substrate gap (Fig. 1c), while for prolonged electrolysis time, the outer diameter of the generated conducting spots exceeded by far the overall SECM tip. These results were explained taking into account the following factors. Firstly, as was outlined above, OH^- produced at the tip impinge on the substrate and cause dissolution of the alumina layer. However, because it is not entirely consumed by the substrate, it can diffuse laterally along the surface and promote further dissolution in undesired regions. Secondly, AlO_2^- formed at the surface of the substrate diffuses outside the tip-substrate gap, where a sharp change in pH (lower than those within the gap) can cause the precipitation of the sparingly soluble and passivating $Al(OH)_3$. This back reaction can also affect the size and the full exposure of the conducting region generated during the base attack of the sample.

To circumvent the above drawbacks, EDTA was used as a scavenger. In fact, EDTA, from one side, can efficiently buffer the solution outside the tip-substrate gap, thus minimising the effect of the lateral diffusion of OH^-. From the other, it can exert its complexing ability towards aluminium ions, forming soluble and rather stable Al-EDTA species [36], thus avoiding the back precipitation of $Al(OH)_3$. The beneficial effect of EDTA as a scavenger is shown in Fig. 4, which displays SECM images of three spots recorded after etching the Pt/Al_2O_3 sample in three different regions, in a solution containing 0.1 M KCl + 0.07 M EDTA + 1 mM $Ru(NH_3)_6Cl_3$. As is evident, in this case, almost circular, but identical platinum spots were recorded. The spots are not perfectly round probably because they reflect the shape and imperfection of the tip (i.e. including the microelectrode and the surrounding insulating sheet) used for those experiments. It must be considered that the alumina film of the Pt/Al_2O_3 sample immersed in the electrolyte solution

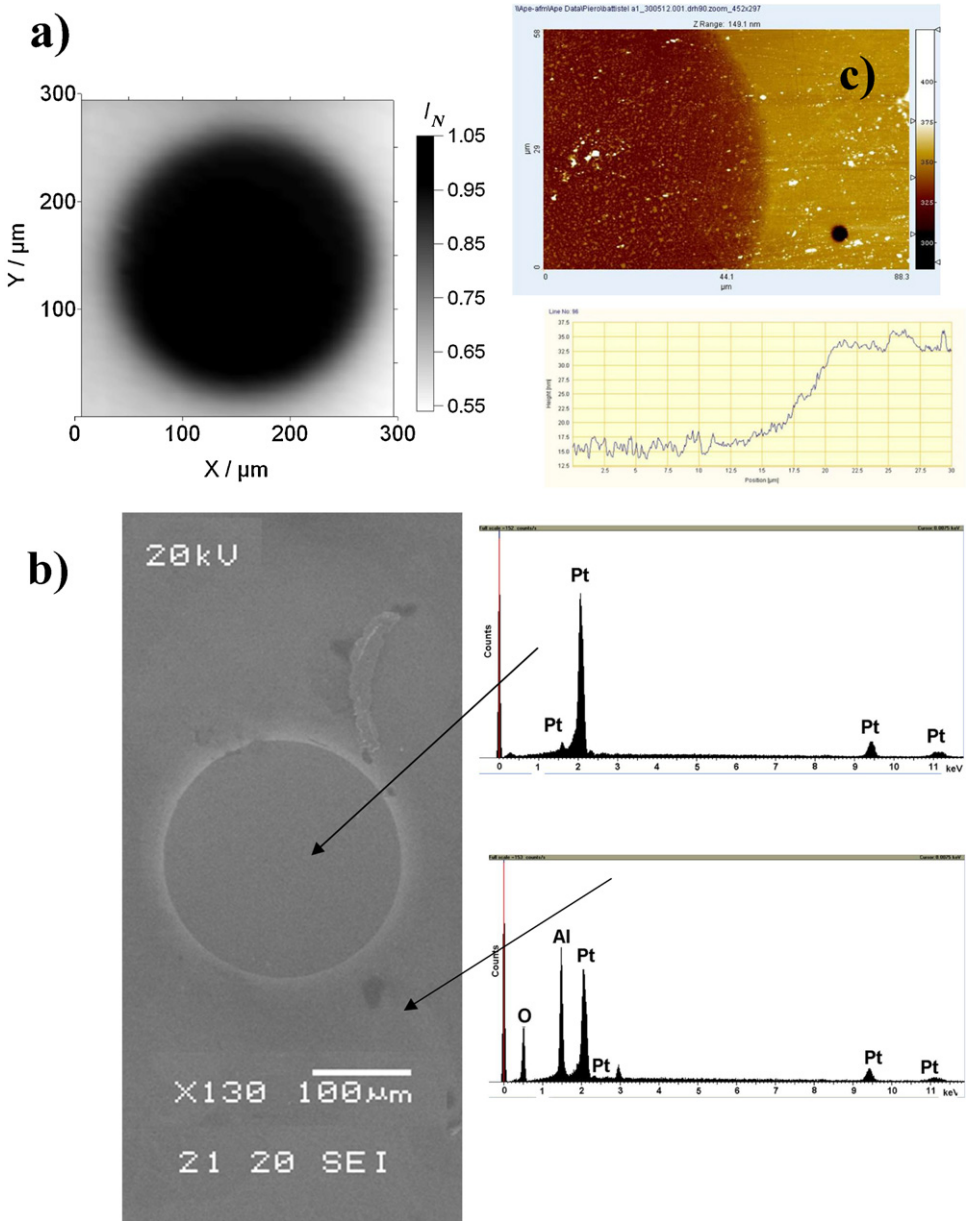

Fig. 5. Comparison of (a) SECM; (b) SEM images recorded after etching the alumina layer and EDS analysis of the etched zone and of the surrounding alumina layer; (c) AFM image of the rim of the Al_2O_3/Pt border and a line scan profile. Experimental conditions as in Fig. 3b.

containing EDTA up to 0.1 M, without base-induced etching, proved to be highly stable. In fact, approach curves and images as those shown in Fig. 1a (filled circles) and b were recorded across the surface, even after the sample had been left in contact with the EDTA solution for 8 h.

The optimum amount of EDTA to add to the solution was established by analysis of the SECM images of at least three repeat etches on different regions of the Pt/Al_2O_3 sample. In particular, the measurements were performed in a series of solutions containing 0.1 M KCl + 1 mM $Ru(NH_3)_6Cl_3$ and EDTA varying from 0.01 to 0.1 M. It was verified that EDTA concentrations over the range 0.07–0.09 M provided platinum spots that were very reproducible, both in size and shape. For instance, a well-defined circular platinum spot, as that shown in Fig. 5a, of about 100 μm was obtained using the electrolyte composition 0.1 M KCl + 1 mM $Ru(NH_3)_6Cl_3$ and 0.07 M EDTA. The latter etches were performed by positioning the 12.5 μm radius Pt electrode at d = 5 μm and using t_{el} = 10 min. The real size of the platinum spots was also verified by SEM-EDS analysis, and Fig. 5b includes, for comparison, a typical image thus recorded. The images obtained by the two different scanning microscopy techniques is amazing good, while, as is also shown in Fig. 5b, the elemental analysis of the spots confirmed the absence of Al in the etched region of the Pt/Al_2O_3 sample.

Based on the above results, in further etching experiments, the concentration of EDTA employed was 0.07 M.

In order to assess the roughness of the etched platinum layer and that of the coating alumina film as well as the sharpness of the transition between the etched platinum and alumina layer, AFM images of the rim of the Al_2O_3/Pt border were taken. Fig. 5c includes an example of such images along with a line scan profile. The root mean square values of about 6 (±2) nm and 4 (±2) nm of the platinum and alumina layer, respectively, indicate that both types of surfaces are smooth. Therefore, topography of these layers could not be revealed by SECM analysis. On the other hand, the AFM line profile suggests that the etched spot has a crater like rim, which extends across about 7 μm, passing from the platinum to the alumina layer.

3.2. Effects of electrolysis time, tip-substrate distance and RG

Fig. 6 shows typical SECM images recorded after base-induced etching of the alumina layer using the 12.5 μm radius Pt electrode (RG = 10), d = 5 μm and t_{el} varying between 2 and 8 min (Fig. 6a), or t_{el} = 6 min and d varying between 1 and 10 μm (Fig. 6b). As expected, both t_{el} and d affected the spot sizes, the letter were larger the electrolysis time or the smaller the tip-substrate distances. In particular, when d = 5 μm it required about 4 min to achieve a platinum

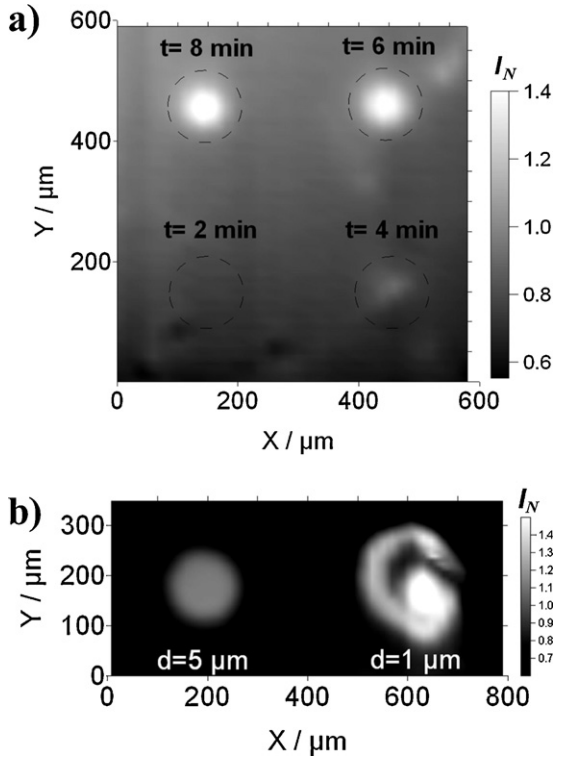

Fig. 6. SECM images obtained after etching the alumina layer for different (a) times or (b) tip-substrate distances (as indicated), using a Pt microdisk 12.5 μm radius (RG = 10), in an aqueous solution containing 1 mM $Ru(NH_3)_6Cl_3$ + 0.1 M KCl + 0.07 M EDTA. Scan speed 10 μm s^{-1}. The etched zones are indicated with circles.

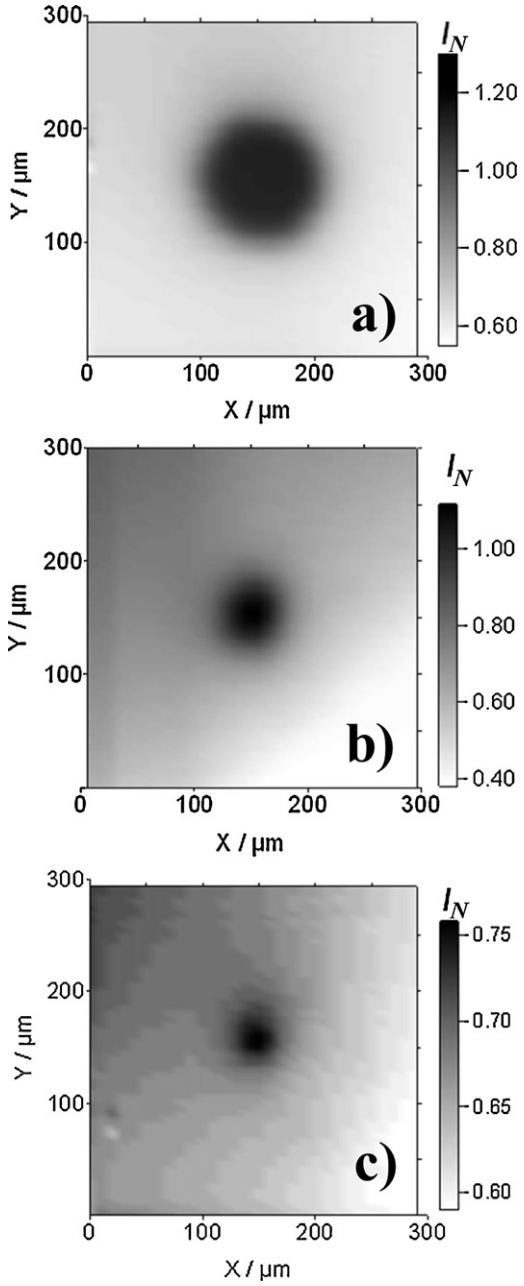

Fig. 7. SECM images obtained after etching the alumina layer for 10 min using various Pt microtips: (a) 12.5 μm radius (RG = 10), (b) 10 μm radius (RG = 5), (c) 2.5 μm radius (RG = 10). Tip-substrate distances: (a) 5 μm, (b) 4 μm and (c) 2 μm. Solution composition same as in Fig. 6.

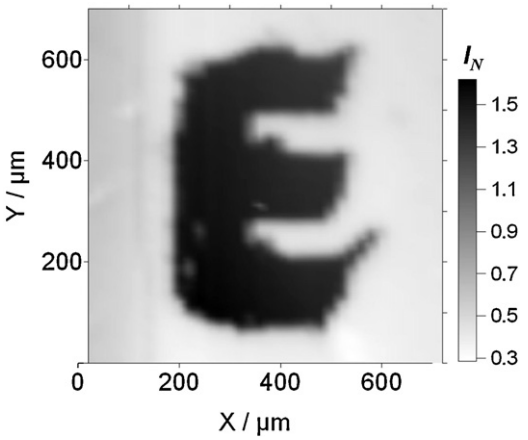

Fig. 8. Letter 'E' written on the Pt/Al_2O_3 substrate using a dynamic wet etching procedure. SECM map obtained by a Pt microdisk 12.5 μm radius (RG = 10) in a solution as in Fig. 6.

spot having the same size of the tip (Fig. 6a), while for t_{el} = 6 min the tip had to be positioned at distances below one time the electrode radius to allow a sensible etching effect. In fact no conducting spot was generated for d = 10 μm. However, when d was relatively low (i.e., d = 1 μm) the shape of the spots was less regular (Fig. 6b). This was probably due to strong convection that originated from hydrogen bubbles formed during OH^- ions production, which made the etchant confinement to within the tip-substrate gap less effective. This problem, apparently, was strongly minimised as soon as the tip was positioned at about 3–5 μm from the substrate (Fig. 6a–b). It is also interesting to note that, keeping the SECM tip at the latter distances, the size of the spots never exceeded the overall tip dimension, even if prolonged electrolysis time were employed. This suggested that resolution of the etching process could be improved by decreasing the RG of the SECM tip. This aspect was investigated by performing etching experiments using two platinum microelectrodes of same radius (12.5 μm), and RG equal to 5 and 10, and using same tip-substrate distance and electrolysis time. Two well shaped circular spots (not shown) were obtained with both microelectrodes and their radii were strictly related to the RG parameters. In fact, the size of the generated spots were equal to about 50 and 100 μm, by using the tip with RG equal to 5 and 10, respectively. Therefore, although the microelectrode active surface area remained constant, the size of the generated spots could be decreased.

Resolution of the etching procedure could also be improved by decreasing either the active area of the microelectrode or the overall tip dimension. As an example, Fig. 7 shows three etches obtained with three microtips of different size, positioned at about 0.4 times of their corresponding electrode radius, and using 10 min electrolysis time. As expected, the size of the conducting spot decreases by decreasing both the active surface area and overall size of the microtip.

3.3. Electrochemical writing

The results obtained in the above sections indicated that using a proper electrolyte solution composition and suitable etching conditions, the Pt/Al_2O_3 sample could be patterned to arrays of platinum disks. Here, we show that more complex patterns can be obtained on the Pt/Al_2O_3 sample by programming the microelectrode tip at a suitable scan rate and tip to substrate distance. As an example, Fig. 8 shows an SECM map of the letter 'E' obtained by etching the alumina layer with a 12.5 μm Pt tip (RG = 10) scanned at 10 μm s^{-1} and positioned at d = 5 μm above the substrate.

4. Conclusions

In this work an SECM procedure for micropatterning alumina thin films has been investigated. It exploits the base-induced dissolution of the alumina layer by local generation of hydroxide ions beneath the SECM tip. The use of EDTA as a scavenger and complexing agent has allowed to strongly improve the reproducibility of the patterns, thus controlling their sizes and shapes. It has also been shown that resolution of the patterns depended on electrolysis time, tip-substrate distance and tip size. The procedure employed here can be used to produce arrays of microelectrodes, which can further be functionalised for application in sensor technology. More in general, the procedure developed here, can be extended for patterning and characterise a variety of alumina-coated metal samples, even with alumina layers ticker than that employed here. In this way conducting microholes, for trapping small volume samples, or microchannels for microelectrochemical devices can be fabricated.

References

[1] S.-C. Hung, O.A. Nafday, J.R. Haaheim, F. Ren, G.C. Chi, S.J. Pearton, Journal of Physical Chemistry C 114 (2010) 9672.
[2] T. Bhuvana, G.U. Kulkarni, ACS Nano 2 (2008) 457.
[3] J. Grunes, J. Zhu, E.A. Anderson, G.A. Somorjai, Journal of Physical Chemistry B 106 (2002) 11463.
[4] D.F. Acevedo, H.J. Salavagione, A.F. Lasagni, E. Morallón, F. Mücklich, C. Barbero, Applied Materials & Interfacesþ V 1 (2009) 549.
[5] S.Y. Chou, M.S. Wei, P.R. Krauss, P.B. Fischer, Journal of Applied Physics 76 (1994) 6673.
[6] L. Rassaei, P.S. Singh, S.G. Lemay, Analytical Chemistry 83 (2011) 3974.
[7] S. Daniele, E. De Faveri, I. Kleps, A. Angelescu, Electroanalysis 18 (2006) 1749.
[8] T. Ito, S. Okazaki, Nature 406 (2000) 1027.
[9] S. Krämer, R.R. Fuierer, C.B. Gorman, Chemical Reviews 103 (2003) 4367.
[10] A.J. Bard, M.V. Mirkin, Scanning Electrochemical Microscopy, Marcel Dekker, Inc., New York, 2001.
[11] A.J. Bard, G.G. Denuault, C. Lee, D. Mandler, D.O. Wipf, Accounts of Chemical Research 23 (1990) 357.
[12] A.J. Bard, L.R. Faulkner, Electrochemical Methods, 2nd ed., Wiley, New York, 2001.
[13] V. Radtke V., C. Heß, J. Heinze, Electrochimica Acta 55 (2009) 416.
[14] D. Mandler, A.J. Bard, Journal of the Electrochemical Society 137 (1990) 1079.
[15] C. Mark, K. Borgwarth, J. Heinze, Advanced Materials 13 (2001) 47.
[16] C. Mark, K. Borgwarth, J. Heinze, Chemistry of Materials 13 (2001) 747.
[17] S. Rapino, G. Valenti, R. Marcu, M. Giorgio, M. Marcaccio, F. Paolucci, Journal of Materials Chemistry 20 (2010) 7272.
[18] C. Cougnon, J. Mauzeroll, D. Belanger, Angewandte Chemie International Edition 48 (2009) 7395.
[19] L. Liu, R. Toledano, T. Danieli, J-Q. Zhang, J-M. Hu, D. Mandler, Chemical Communications 47 (2011) 6909.
[20] F. Deiss, C. Combellas, C. Frétigny, N. Sojic, F. Kanoufi, Analytical Chemistry 82 (2010) 5169.
[21] N. Ktari, S. Nunige, A. Azioune, M. Piel, C. Connan, F. Kanoufi, C. Corbellas, Chemistry of Materials 22 (2010) 5725.
[22] S. Meltzer, D. Mandler, Journal of the Chemical Society, Faraday Transactions 91 (1995) 1019.
[23] C. Bragato, S. Daniele, M.A. Baldo, G. Denuault, Annali di Chimica 92 (2002) 153.
[24] C-A. McGeouch, M.A. Edwards, M.M. Mbogoro, C. Parkinson, P.R. Unwin, Analytical Chemistry 82 (2010) 9322.
[25] M. Sheffer, D. Mandler, Journal of Electroanalytical Chemistry 622 (2008) 115.
[26] R. Cornut, S. Nunige, C. Lefrou, F. Kanoufi, Electrochimica Acta 56 (2011) 10701.
[27] C. Heß, K. Borgwarth, C. Ricken, D.G. Ebling, J. Heinze, Electrochimica Acta 42 (1997) 3065.
[28] Y. Zu, L. Xie, B. Mao, Z. Tian, Electrochimica Acta 43 (1998) 1683.
[29] J. Ufheil, C. Heß, K. Borgwarth, J. Heinze, Physical Chemistry Chemical Physics 7 (2005) 3185.
[30] V. Radtke, C. Hess, R.M. Souto, J. Heinze, Zeitschrift fur Physikalische Chemie 220 (2006) 393.
[31] D. Battistel, S. Daniele, R. Gerbasi, M.A. Baldo, Thin Solid Films 518 (2010) 3625.
[32] A.I. Oleinick, D. Battistel, S. Daniele, I. Svir, C. Amatore, Analytical Chemistry 83 (2011) 4887.
[33] D. Battistel, S. Daniele, G. Battaglin, M.A. Baldo, Electrochemistry Communications 11 (2009) 2195.
[34] I. Ciani, S. Daniele, Analytical Chemistry 76 (2004) 6575.
[35] J.L. Amphlett, G. Denuault, Journal of Physical Chemistry B 102 (1998) 9946.
[36] R.J. Motekaitis, A.E. Martell, Inorganic Chemistry 23 (1984) 18.